



From untangled graphs and nets to tangled materials

Stephen T. Hyde*, Olaf Delgado Friedrichs

Applied Maths Department, Research School of Physics, Australian National University, Canberra, ACT 0200, Australia

ARTICLE INFO

Article history:

Received 13 April 2010

Received in revised form

19 October 2010

Accepted 21 October 2010

Available online 11 November 2010

Keywords:

Entanglement

Knotted graphs

DNA materials engineering

Metal-organic frameworks

ABSTRACT

We suggest constructive definitions for the determination of untangled finite graphs and three-periodic nets, using barycentric embeddings in two and three dimensions. The possibility of deliberately constructing tangled graphs and nets is canvassed, and we conclude that tangled patterns offer a novel class of nano- and meso-structured materials with useful features, including high internal surface area and volume and chirality.

Crown Copyright © 2010 Published by Elsevier Masson SAS. All rights reserved.

1. Introduction

Osamu Terasaki has made a consistent impact on the study of nanoporous and mesoporous materials. His masterful use of the electron microscope to unravel complex structures is well documented. To relative outsiders such as us, the importance of his work lies beyond the technical brilliance of his microscopy. Rather, Osamu's detailed observations and structural reconstructions reveal the truth of an important article of faith to all materials scientists: structure plays *the* central role in the behaviour and design of materials. He shields closet geometers from the increasingly frequent catcalls by the real outsiders, who fail to recognise an essential difference between science and engineering. Without your work, we would have little defence against the charges of “uselessness”: Osamu, we need you!

2. Structural entanglement

With that defence of our own position out of the way, we feel able to assert the relevance of a topic that remains scarcely touched to date in porous materials research: that of *structural entanglement*. Our principal goal in this paper is to describe in very crude general terms the concept of entanglement and to suggest a possible first step towards a characterisation of (dis)entanglement in *graphs* and *nets*. Graphs correspond to the structures formed by finite ‘molecular’ networks, with a bounded number of vertices. In contrast to finite graphs, infinite nets are crystalline

networks and contain an infinite number of vertices. They can be two- or three-periodic, with 2D or 3D unit cells respectively; we usually use the term to describe three-periodic examples.

So far, entanglement has been recognised and discussed to some degree by scientists interested in a somewhat different class of porous materials to porous inorganic materials championed by Terasaki and his colleagues: metal coordination polymers (or metal-organic frameworks, MOFs).

The structural richness of entangled, catenated and/or knotted patterns has long been a target for synthetic organic chemists. Knotted molecules were first prepared by Dietrich-Buchecker and Sauvage [1]. Since then, numerous other examples have been found. Catenated organics are an equally rich area, including catenanes and rotaxanes [2].

MOFs are built from polymeric edges, condensed to form nets by coordinating metal ions. In a sense they are giant floppy analogues of classical covalent frameworks, such as zeolites. It is this floppiness, inherited from the polymeric ligands, that admits the possibility of tangled structures. The edges may well wind around each other before or during their condensation into nets, resulting in structures that may be – qualitatively at least – tangled. As first pointed out by Robson and Hoskins [3], numerous MOFs display complex and various forms of entanglement, discussed in some detail in a rich review by Proserpio *et al.* [4]. In this review, the authors also pointed out that many MOFs can be considered as catenated nets, whose types of catenation can be to some extent explained by exploring the threading of various rings in the structures. That is a useful approach in that it allows for the threading to be classified according to the mathematical *links* formed by the threaded rings.

* Corresponding author.

E-mail address: stephen.hyde@anu.edu.au (S.T. Hyde).

One particular example of a MOF [5] consists of a triplet of “chicken-wire” nets (or, using O’Keeffe’s notation, *hcb*, [6]), intergrown to form arrays of Borromean rings. Proserpio *et al.* reinterpreted the structure to include neighbouring Ag–Ag interactions as net edges [4]. The resulting structure is a degree-four network, built of six-rings, whose *topology* is identical to that of the diamond (*dia*) net. If the geometric location of the nodes in the net is ignored and the net is considered as a topological *graph* only, the structure is indeed *dia*. However, the net is very different to *dia*, in that the crossing of edges viewed from various directions is distinct to that of *dia*. This situation is analogous to the formation of a knot from a simple loop of string that is wound up to give a multiple loop. A knot results when the under-over crossings of the loop are changed from those that can be formed by simply winding up the loop, for example by rethreading a loose end through the loop.

This phenomenon is perhaps most simply explained within the language of mathematical graph theory. A graph is a topological entity only; its structure is nothing more than the connection table of edges. Since topology is only concerned with the linkages between vertices, vertex and bond locations in space are irrelevant. For example, the (complete) graph, K_4 , contains just four vertices, and each vertex is connected to each other (so all vertices have degree-three). There are an infinite number of different ways that this graph can be *embedded* in space, all of which preserve the graph topology. We can therefore construct an infinite variety of K_4 graphs in space, all topologically equivalent, despite their possibly distinct spatial *embeddings*. Some examples are shown in Fig. 1.

Among topologically equivalent nets, two levels of structural flexibility remain. The first is the usual geometric placement or embedding of the graph, described for example by the cartesian coordinates of the vertices. If two embeddings of K_4 can be matched (possibly after a rigid-body rotation and translation) to each other, they are congruent. Here, the notion of matching is important. If one assumes that the bonds are – for example – straight edges linking vertices, congruence is measured by vertex locations alone. Imagine, however, that the bonds themselves are free to wander through space. Strict congruence between a pair of K_4 embeddings then

demands that all of the points of space occupied by these particular embeddings can be overlaid, including edges as well as vertices.

For many purposes, strict geometric congruence is too restrictive. For example, if edges are displaced a little, the net remains for most purposes essentially unchanged. However, if edge displacements are so large that edges are forced to pass through each other during bending, their mutual threading in the structure changes, even while their topology remains unchanged. To account for the possibility of various entanglements, a second form of structural equivalence – more restrictive than topology but less so than geometry – is worth considering.

This intermediate taxonomy of nets – somewhere between topology and geometry – recognises that among all topologically equivalent structures, various entanglements are possible. How do we classify these? The situation is strongly reminiscent of knots, where it can be very difficult (if not impossible) to decide if two windings are equivalently knotted. If they can be morphed into each other without edges having to pass through each other, they are demonstrably equivalent knottings. Mathematicians refer to embeddings that are equivalent within an arbitrary spatial rearrangement of the vertices and edges that are not change the crossings as lying within the same *ambient isotopy* class.

All structures that can be morphed into each other without edges crossing through each other en route are (in our terminology) equivalent *isotopes*. Just as it is generally difficult to decide whether two tangled loops of string are essentially the same knot, it is a challenging question to decide if two graph or net isotopes are equivalent. Some simple questions that emerge when thinking about this problem:

- When is a net *tangled*?
- Are tangled nets necessarily knotted?
- Are knotted nets necessarily tangled?

In this paper, we will discuss some introductory observations concerning those issues; they are by no means conclusive, but show that the topic is a rich one, worth serious thought.

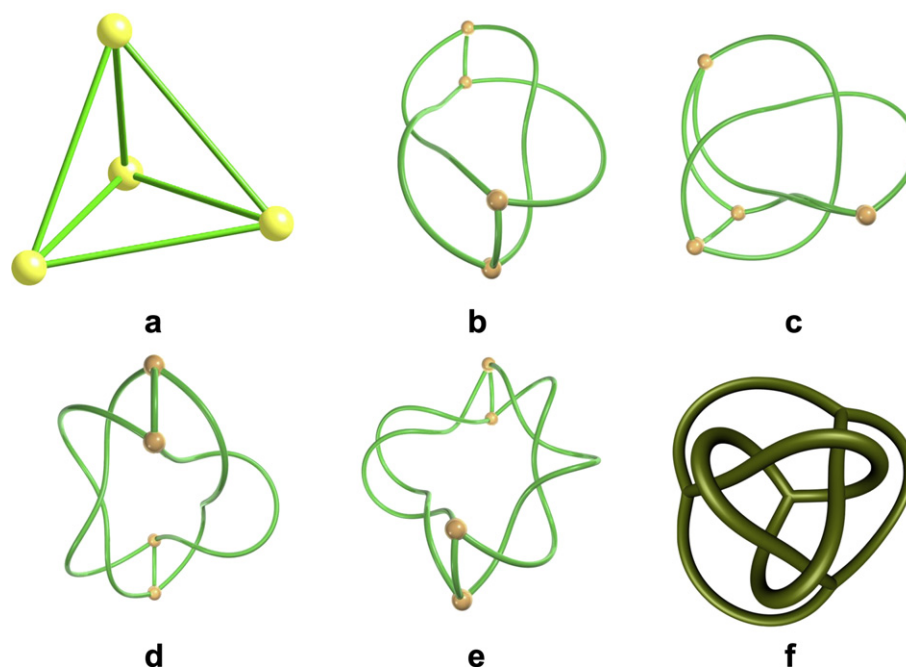


Fig. 1. Six distinct embeddings of K_4 , the graph of edges of the tetrahedron. All are topologically equivalent, yet all differ in the mutual weaving of edges. (a) is the usual untangled tetrahedral embedding, (b–f) are tangled. (b–e) contain knots and/or links and are therefore also knotted, whereas (f) is unknotted. We call these distinctly tangled embeddings distinct *isotopes* of K_4 .

3. Tangled frameworks: playing with ambient isotopy

To explore these questions, it is helpful to think first of the analogous – and we shall see, simpler – question of a taxonomy of knots. Knot theory has undergone a resurgence in recent decades driven by the power of the Jones polynomial and related polynomials that offer powerful algebraic tools for distinguishing different knots and links (i.e. distinct isotopes of a simple loop, or multiple loops). This knot invariant approach hopes to provide a characteristic equation of knots, thereby rendering the issue of knot taxonomy to one of algebra.

More recently, an alternative approach has been explored, that appeals immediately to geometry rather than algebra. This approach seeks to find a canonical embedding for each isotope. If such a route could be found, and if that embedding were unique, the difficult algebraic question as to whether a pair of knots are the same isotope or not is answered by relaxing each knot to a canonical form and then checking if they are geometrically equivalent or not. This geometric approach is attractive (though, like the algebraic route, it remains incomplete).

In fact, if we are looking only to distinguish different net *topologies* (rather than isotopes of the same net topology), the geometric approach is powerful and easily implemented. A simple route is to form a canonical “equilibrium placement” [7]. This placement is described by crystallographic coordinates for the vertices, which are then joined by straight edges. The coordinates are precisely those formed by barycentric placement, where each vertex is at the centre of mass of its immediate neighbouring vertices (one edge distant). We can give that abstract crystallographic placement an explicit spatial geometry by choosing a unit cell size and shape, and locating the vertices at cartesian coordinates corresponding to the crystal coordinates. The resulting net whose embedding is that due to equilibrium placement (described in [7]), is unique and therefore affords a canonical geometrisation for a given net topology. In some cases, the algorithm produces ‘collisions’ where edges of the systre net can cross through each other.

Note, however, that the equilibrium placement approach does not give a canonical geometry for isotopes, since distinct isotopes of the same topology will all relax to the same net. However, we will make the case in this paper that equilibrium placement also offers a convenient tool for determining an untangled isotope of a graph or net.

4. Baby steps towards quantification of entanglement

4.1. Knots in untangled frameworks

A natural starting point in any investigation of tangled graphs and nets is the domain of knots. However, all (three-periodic) nets

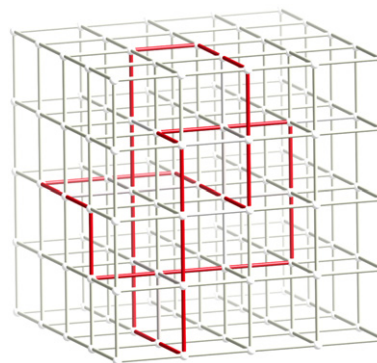


Fig. 2. An examples of a knot within the untangled embedding of the *pcu* net: the four-crossing figure-of-eight (4_1) knot.

contain knots and links in profusion. Look for example at the net that arises by tiling space with face-sharing cubes, whose edges form a simple-cubic net, shown in Fig. 2 (called, in the jargon of O’Keeffe’s three-letter codes for nets, *pcu* [6]).

This embedding must surely be characterised as the untangled isotope among all nets with the same topology as *pcu*. Indeed, the barycentric embedding of the *pcu* topology gives this embedding. Notice that the smallest cycles in the graph – the four-sided rings surrounding cube faces – are unthreaded. However, generic closed loops in the *pcu* net give various knots. For example, a 24-edge cycle in the *pcu* net is sufficiently large to form the trefoil, the simplest knot. An example of a cycle that gives the 4_1 knot is shown in Fig. 2, adapted from [8].

The possibility of knots in untangled nets is unsurprising, given the arbitrarily large cycles than can be traced in nets. A less evident possibility is the following. Some graphs and nets contain knots and or links formed by their shortest cycles. For example, Conway *et al.* showed that *all* possible embeddings of the complete graph with 6 vertices (K_6) in three-space necessarily contains interlinked loops among the set of triangular cycles [9]. An example is shown in Fig. 3 (b). It is therefore useless to attempt to define untangled isotopes of nets as those free of knots or links.

The unavoidable threading seen in K_6 is also found in infinite nets. That observation is, in isolation, uninteresting, but are those links formed by smallest cycles in the nets? Are all these cycles unknotted and unlinked in an untangled net? Clearly, the answer is yes in some cases (e.g. *pcu*, cf. Fig. 2). But in other cases – analogous to the situation of K_6 – this requirement cannot be satisfied. Intriguingly, this situation arises for example in the high-pressure polymorph of silica, coesite (or, in the nomenclature of [6], *coe*), shown in Fig. 3. The smallest cycles (or “strong rings” [10]) of the coesite framework form links that cannot be unthreaded, no matter

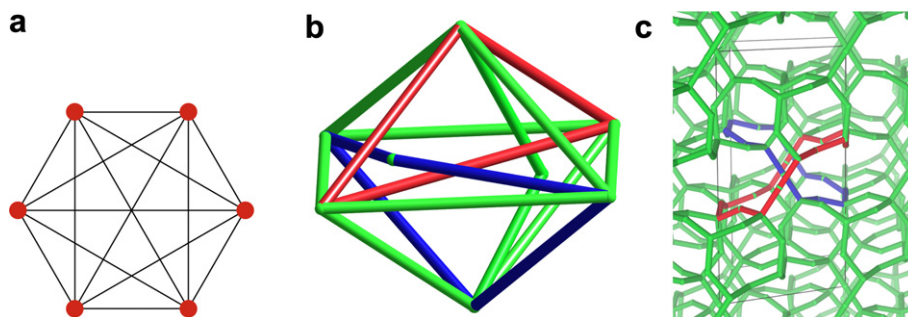


Fig. 3. (a) Planar drawing of the complete graph, K_6 , with vertices marked by red dots. (b) One 3D spatial embedding of this graph with the six vertices located as in an octahedron; red and blue cycles are threaded. Any spatial embedding of this graph results in a link [9]. (c) A barycentric embedding of the coesite net, with linked strong rings highlighted as red and blue cycles (For interpretation of the references to colour in this figure legend, the reader is referred to the web version of this article).



Fig. 4. Distinct cycles in the ravelled tetrahedron of Fig. 1(f), highlighted in red. (All other loops in the figure are related by the three-fold symmetry of the ravel to one of these two loops.) None of these cycles is knotted (For interpretation of the references to colour in this figure legend, the reader is referred to the web version of this article).

how the edges are rethreaded in the network. It is likely that knotting in this case is induced by the high density of the net.

So we are faced with a potential dilemma in defining the untangled state of the *coe* net. Either all isotopes of the coesite net topology are classified as tangled due to the presence of these links, or we choose a specific isotope among all those isotopes topologically equivalent to coesite as the untangled embedding. In our view, the latter is a better choice. However, we must then accept that *entanglement* is a distinct entity to *knottedness*. In particular the coesite example shows that untangled nets can nevertheless contain knotted or linked cycles, even among their shortest cycles, defined by the strong rings of the net.

4.2. Tangled but unknotted nets

Stranger still, we can find examples of tangled nets, whose shortest loops are all unknotted. In a recent paper, we called this mode of entanglement a *ravel* [11] (These have also been discussed in the mathematical literature, and the earliest report known to us is by Kinoshita [12]. Other authors have called these patterns ‘almost unknotted’ graphs [13]). Ravelled nets can be totally free of knots, but they cannot be classified as untangled. A simple example can be formed in the complete graph with four vertices (K_4). Surely the untangled isotope of K_4 is that formed by the edges of the usual tetrahedron. So the ravelled isotope of K_4 shown in Fig. 1(f) is necessarily tangled. But all cycles in this isotope are themselves unknotted, as shown in Fig. 4.

We can think of the K_4 graph as a branched knot, and that branching (induced by the degree-three vertices) evidently complicates the problem of entanglement to a level beyond that found in knots (which, by definition, are tangled isotopes of vertex-free loops). This idea can be generalised; for example, a suite of tangled symmetric patterns for branched vertices of degree 2, 3 and 4 are illustrated in Fig. 5(b–d). These patterns are nothing more than branched cinquefoil (five-crossing) knots Fig. 5(a). Knotted or unknotted cycles result from these patterns, depending on how the loose ends are connected, as shown in Fig. 5(e–g). Knots (such as the cinquefoil) then, are merely the simplest possible mode of entanglement of a graph or net. But they are neither necessary nor sufficient for a net to be tangled or untangled!

Related tangles are easily formed from these examples, such as the tangle shown in Fig. 6(a). This ravel – while tangled – has no knotted cycles (and is called a *universal ravel* [11]). It can therefore be inserted into an unknotted net (thereby tangling the net) without adding knots, by replacing a star of edges radiating from a single vertex by the ravel, as in Fig. 6(b). The resulting net is knot-free (Fig. 6(c,d)). It is also link-free (since links are defined only for disjoint cycles). Note, however, that if shortest cycles spanning all angles in the net are included, a pair of cycles, sharing a common vertex, are threaded (Fig. 6(e)).

The detection of tangled nets is therefore a complex problem. Significant progress has been made in numerical detection of knots and links in structures, prompted by Proserpio *et al.*'s observations on entangled MOFs. In particular, Blatov has authored the *TOPOS*

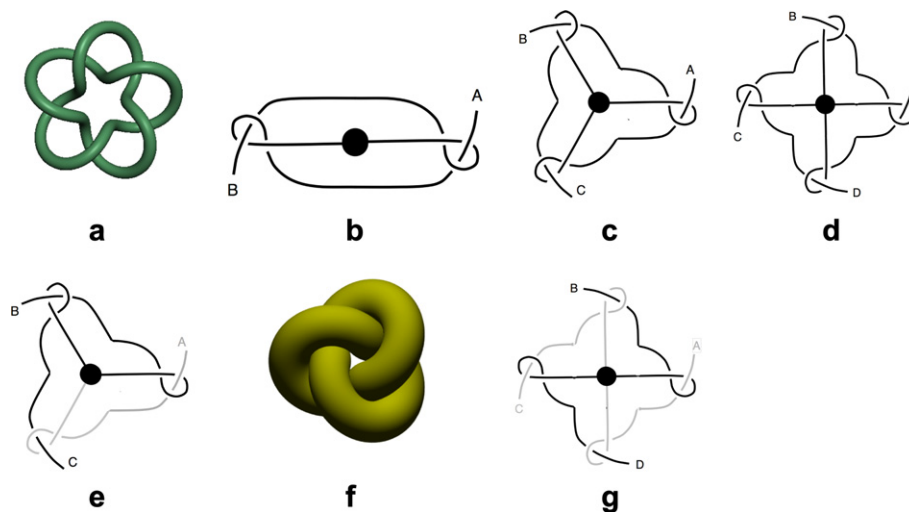


Fig. 5. (a) The cinquefoil knot, a five-crossing knot. (b–d) Sequence of analogous tangles of increasing vertex-degree. (b) is an identical isotope to the cinquefoil, while (c–d) show related tangles formed by forming 3- and 4-fold rotationally symmetric patterns from the 2-fold pattern. (e) If any pair of adjacent loose ends in the 3-, 4- ...-fold tangles are joined (such as the ends at B and C in (c)), a trefoil knot results. (f) The trefoil knot. (g) If next-to-adjacent loose ends are joined (e.g. B and D of (d)), the pattern is knot-free, yet tangled. We call this latter feature a “ravel”, cf. [11].

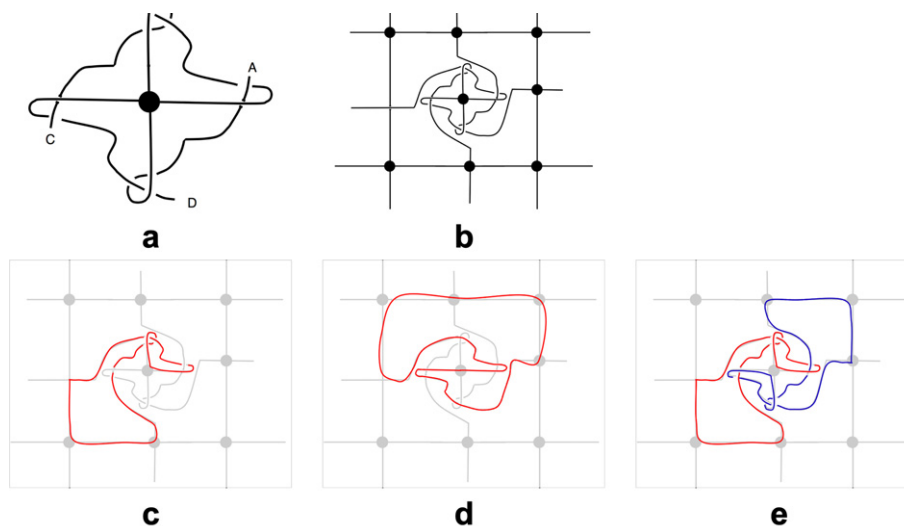


Fig. 6. (a) A universal ravel. (b–c) Connection of any pairs of dangling ends gives an unknotted loop. (d) This example does contain threaded cycles, sharing a common vertex.

software package, for detection of these entanglement modes in nets [14]. This approach is an excellent start to this problem, but current versions, which rely on numerical detection of threading of disjoint loops, fail to detect ravels.

An open question emerges from the observation that ravels allow entanglement without the presence of knots or links: namely, are there yet more entanglement modes that are both ravel- and knot-free? Indeed is there an infinite hierarchy of entanglements, of which knots (tangled loops) and ravels (tangled vertices) are the simplest? If the answer is affirmative, we remain a long way distant from understanding of tangling in nets, let alone possible classification of tangles in nets.

4.3. A tentative definition of the untangled isotope for a given net topology

Though the choice of the untangled ‘ground state’ isotope for a graph or a net is arbitrary, it would be helpful to arrive at a definition that produces the ‘usual’ isotopes of well-known graphs or nets. The exercise is, however, less clear cut than the choice of the untangled knot (or unknot), which is clearly a simple uncrossed loop. The previous examples show that any attempt to align the notion of an untangled net with the presence of knots and or links is flawed, since entanglement can occur in the absence of knots, and knots can occur in the absence of entanglement. Of course, all such discussion is predicated on a firm understanding of what constitutes entanglement.

A graph, with a finite number of vertices, is fundamentally distinct from a (three-periodic) net, due to the unboundedness of the nets. We may hope to reduce the study of nets to that of graphs, via (for example) the concept of ‘quotient graphs’, introduced by Chung *et al.* [15]. This construction is analogous to the reduction of an infinite crystal to a single unit cell, coupled with periodic boundary conditions. While this approach is useful for understanding the topologies of nets, it cannot encode the threading of loops in nets faithfully, since loops may extend beyond a single unit cell of the net. Further, the ‘gluing’ of vertices separated by a lattice vector implicit in the quotient method introduces spurious cycles. In other words, the quotient graph is a very different isotope to the original three-periodic net. This difficulty with (infinite) nets places them in a distinct category to (finite) graphs; we deal with the characterisation of their untangled isotopes separately below.

4.4. Untangled isotopes of planar and polyhedral graphs

The definition of an untangled isotope for some classes of graphs is clear. For example, planar graphs can be drawn on the page without edge crossings. Since this drawing can be seen as (e.g. stereographic) projection from the sphere onto the plane, they also reticulate the sphere. Therefore polyhedral graphs, which are simple, planar and 3-connected – such as the graph of edges of polyhedra – lie in the sphere. (“3-connected” graphs are those that cannot be split into multiple disjoint graphs by removal of less than 3 vertices and accompanying edges. It does not refer to the number of edges incident to a vertex, that we call here the vertex “degree”.) Further, Whitney proved that there is only one way to embed a 3-connected planar graph in the plane or sphere, so the isotope of any polyhedral graph that lies on the sphere is unique [16].

Topologists speak of the “minimal genus embedding” of a graph, that is the lowest genus surface (strictly, a 2-cell embedding of an oriented 2-manifold) which can be reticulated by the graph, without edge crossings (for details, see, for example, [17]) (This is also sometimes referred to as the “graph genus” or the “cyclomatic number” of the graph). Thus, the minimal genus of polyhedral graphs for example is zero, and if an isotope of a polyhedral graph cannot be embedded in a sphere, it is tangled. Indeed, we have used this as a guide to enumerating tangled polyhedral graphs: we assume that the simplest tangled isotopes reticulate the (genus-one) torus rather than the (genus zero) sphere [18,19].

This topological criterion is our preferred starting point for understanding tangled graphs. So what of more general graphs? It is reasonable to demand that an untangled isotope of a particular graph reticulate a surface whose genus is the minimal genus of the graph; conversely if an isotope can only be embedded in a surface of higher genus than the minimal genus it is necessarily tangled.

Consider, for example, the complete graph with six vertices, K_6 , shown in Fig. 3. This cannot reticulate the sphere, therefore an untangled isotope of K_6 will exhibit more threading than untangled isotopes of polyhedral graphs. There are four distinct ways of reticulating the torus to form K_6 [20], so the untangled isotope of K_6 is among these examples. In fact, it turns out that all of these ‘toroidal isotopes’ are equivalent, even though they reticulate the torus in distinct ways. The spatial embeddings that result from these four torus embeddings – assuming the usual donut-shaped embedding of the torus in space – can be deformed into each other

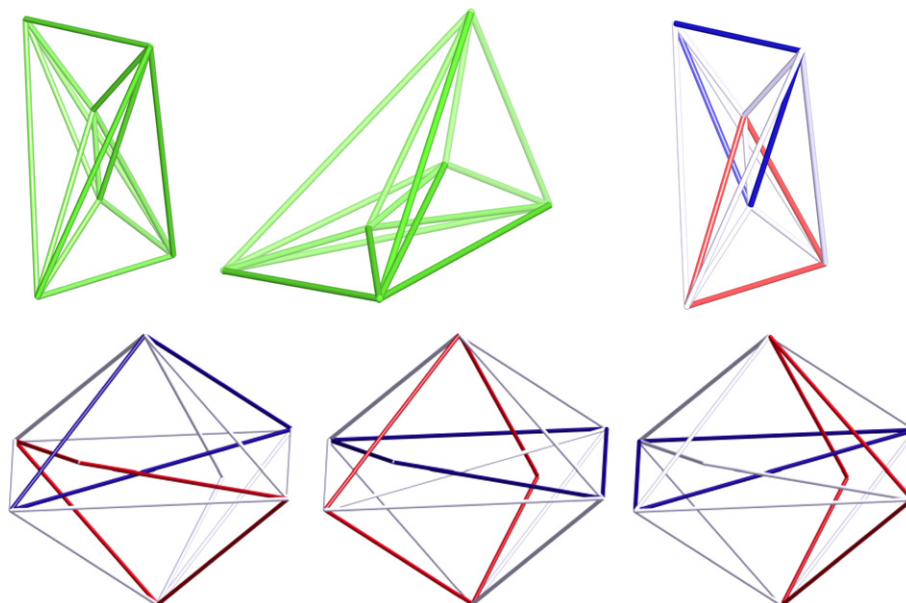


Fig. 7. Top left and middle: Two views of the untangled isotope of K_6 . Top right: This isotope contains a single Hopf link formed by a pair of the triangular cycles in the net. Bottom: Three distinct Hopf links formed by pairs of triangular cycles in a tangled isotope of K_6 .

without forcing edges to pass through each other. Therefore all four toroidal embeddings yield the same isotope in 3D space. Since the torus is the lowest genus orientable manifold that can be reticulated by K_6 without crossings on the surface, this isotope qualifies as the untangled isotope of K_6 . A view of this isotope is shown in Fig. 7. Indeed, this isotope is partially threaded: it contains a single (Hopf) link between disjoint triangular rings, shown in Fig. 7. Despite this unavoidable threading, the untangled K_6 isotope is less threaded than tangled counterparts. For example, the isotope shown in Fig. 3 contains a number of (Hopf) links, illustrated in Fig. 7.

This minimal genus criterion is necessary, but may be insufficient to characterise the untangled isotope, since there may be a number of isotopes that share this same minimal genus surface. In contrast to the K_6 example, in general the various reticulations of minimal genus 2D manifolds of a graph will result in distinct isotopes in 3D space. A further step is then necessary to isolate the untangled isotope. We propose a geometric approach to choose an untangled isotope in these cases. Consider first the situation where the relevant minimal genus embedding is the torus. In those cases, the various reticulations on the torus by the graph can be lifted to a simple two-dimensional euclidean net by mapping the reticulation onto its *universal cover*. This step amounts to an unfolding of the torus into the plane to form a single 2D unit cell. The complete universal cover is a infinite 2D crystalline pattern, where each unit cell of the 2D net corresponds to a single copy of the antecedent torus (The universal cover is described in many texts, e.g. [21]). The manner in which edges of the net decorate the torus are encoded in

the universal cover via their directions with respect to the pair of lattice vectors defining the unit cell, in much the same way as a helix winding a cylinder can be indexed according to its pitch relative to the cylinder axis, or equator. Thus, heavily wound edges on a torus have high indices. This means that the edge lengths in the universal cover – for a normalised cell area – are a gauge of the degree of winding of the edges. Alternatively, if the average edge length is normalised (to one, say), the area of the unit cell varies inversely with the degree of winding of edges. Therefore, large unit cell area imply simpler entanglements. Of course, there are many degrees of freedom in this universal cover, corresponding to the many possible tori. Among those possibilities, we choose a cell that has largest area consistent with (i) barycentric embeddings (i.e. 2D equilibrium placement) and (ii) average edge length of one. Barycentric coordinates are optimal for our purposes, since these lead to minimal squares of the edge lengths compared with any other embedding with the same topology as those of the universal covers [7].

This prescription is precisely that used by the *Systre* software for finding canonical embeddings for 3D and 3D nets, making this calculation straightforward in cases where the minimal genus of the graph is one [7,22]. For example, consider the four distinct reticulations of K_6 on the torus [20]. These reticulations lift to universal covers whose barycentric embeddings are shown in Fig. 8 (Recall that this calculation is technically unnecessary in this case, as all four reticulations give the same isotope. We show this example here to illustrate the technique only). Barycentric embeddings of the universal covers result in unit cells with four and six vertices for these examples. To compare the area of each

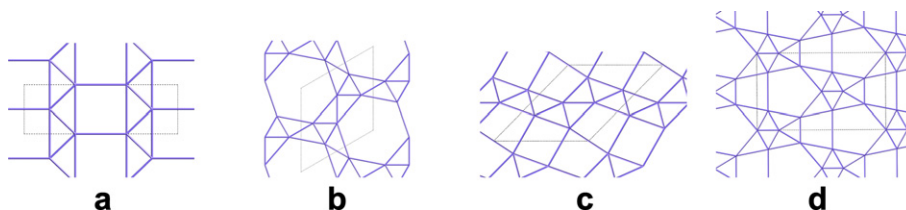


Fig. 8. Barycentric embeddings of the four toroidal reticulation of the K_6 graph. The unit cell of the first pattern contains four vertices (an artifact of the analysis that for convenience treats all vertices as alike, a single copy of the graph contains six distinct vertices).

Table 1
Unit cell dimensions for barycentric embeddings of the four toroidal reticulations of K_6 shown in Fig. 8 with average edge lengths set to unity.

Pattern	a	b	γ	# of vertices	Normalised area
(a)	3.50126	1.11084	90	4	5.8340
(b)	2.78924	2.78924	120	6	6.7376
(c)	3.03554	2.71614	45.45	6	5.8709
(d)	2.72667	4.59082	90	6	6.2588

domain corresponding to a single torus, we scale the area to accommodate the six vertices in K_6 , resulting in the normalised areas listed in Table 1. These areas are those of largest (flat) tori whose reticulations have average edge lengths of one. Since embedding 2 has the largest area in the universal cover corresponding to a single copy of K_6 in the torus, this is the best candidate for the untangled isotope according to the working definition proposed above.

With this prescription, the determination of the untangled isotope for genus-one cases is straightforward.

4.5. Untangled isotopes of higher genus graphs

In principle, a similar approach is feasible for higher genus graphs also. However, once the minimal genus exceeds one, the universal cover lies in the hyperbolic rather than the euclidean plane. A numerical algorithm to form barycentric 2D hyperbolic patterns has yet to be developed, though we see no conceptual obstacle to extending the euclidean process to hyperbolic space.

4.6. Untangled isotopes of 3D nets

If the graph is infinite, such as periodic (3D) nets, the approach described above fails, since a single copy of the net in its universal cover has infinite area in the hyperbolic plane. Simplification of the net to a finite graph, such as the quotient graph, also fails to capture the essential features of the isotope, for reasons outlined in Section 4.3 above. We propose a slightly different algorithm for the determination of the untangled isotopes of nets, but one that again calls on equilibrium placement. In this case however, the calculation is done in 3D euclidean space, rather than within the space containing the universal cover of the 2D reticulation. Ironically, the situation is more straightforward for infinite nets than for finite graphs! The prescription for nets is simple: the untangled isotope is

equivalent to that formed by the barycentric embedding in 3D euclidean space. Though this abstract placement is not a metric embedding of the net, imposition of any metric (i.e. unit cell vectors) will result in the same isotope. Therefore, we define the untangled isotope of a (collision-free) net to be that given by equilibrium placement. Conversely, distinct isotopes of the net, with different edge crossings, are *tangled*.

This working definition of an untangled net shares some feature of the unknot. In particular, it has an isoperimetric property that is reminiscent of the unknotted loop: it minimises the squares of edge lengths for a fixed cell volume [7]. This observation was noted earlier: Delgado Friedrichs and O’Keeffe remarked that barycentric embeddings are appealing in that they avoid “unnecessary entanglements” [7].

We note that this definition fails for nets whose equilibrium placement results in vertex collisions. That remains an open problem. Indeed, it appears to be likely that net topologies with collisions may have more than a single untangled isotope under any reasonable definition of the untangled isotope.

The algorithms presented here for untangled isotopes are explicitly geometric, and hence constructive. We find this a distinct attraction of the approach, but we do not claim that the issue is now firmly resolved. It is worth pointing out here that at least one other definition has been proposed, namely that untangled isotopes are characterised by minimal crossing number, averaged over of all possible planar drawings of the graph [13]. In the case of polyhedral graphs, this criterion very likely coincides with that of minimal genus. For more complex graphs, we prefer to generalise the concept of a 2-manifold reticulation, and define the unknotted isotope to be that which reticulates a manifold of simplest topology (lowest genus) and largest cell volume in the universal cover. Does this isotope afford the minimal crossing number? We do not yet know.

5. Tangled materials

5.1. Metal-coordination polymers, DNA assemblies and mesoporous materials

This topic is a very attractive and rich one at a theoretical level, but is it of any interest to the materials chemist? The recognition of tangled motifs in actual materials is recent, and to date is largely confined to some examples of MOF’s, as described in Section 2. That tangled patterns are formed in these materials, whose net edges are

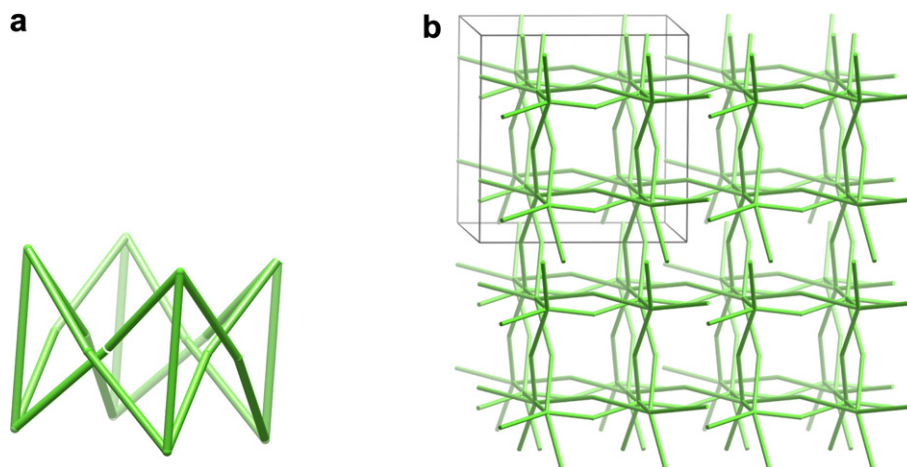


Fig. 9. (a) A toroidal “wreath” isotope of the cube graph. Vertices have been displaced from those of the usual (untangled) cube to reduce the edge crossings and to highlight the chirality of the isotope. Assembly of these tangled cubes into a simple-cubic lattice gives a tangled and chiral *pcu* net (cf. Fig. 2). Figure adapted from [18].

polymeric ligands, is unsurprising. In our view, it is certain to recur in materials whose ligands are extended and flexible. Though we have seen above that entanglement is a more general phenomenon than knotting, it is known that polymer chains exhibit an increasing tendency to knot as their length grows [23]. Therefore graphs whose edges are polymer chains are also likely to be entangled if the edges of the graph are sufficiently long compared with the characteristic length of the polymer.

A promising class of network materials are those built by self-assembly of DNA strands, pioneered by Seeman (see, for example, [24]). These materials afford very efficient yields of prescribed topologies, due to the specific recognition of complementary base pairs of DNA. Both extended networks and polyhedral graphs have been synthesised from strands of DNA [25–27]. Though DNA is a relatively stiff polymer, it can readily form knots, provided the strands are sufficiently long [28,29]. Assembly of tangled graphs and nets is therefore likely once the edges are sufficiently long.

Indeed, Hanadi Sleiman has confirmed that assembly of polyhedral graphs results in a 100% yield of the desired (untangled) pattern, except for larger molecular weight ligands [30]. It is likely that the less-than-perfect yield for larger polyhedral structures is due to the formation of tangled polyhedral graphs, whose simpler representatives are the toroidal examples discussed elsewhere [18,31]. A similar phenomenon is likely to be found also in extended framework nets constructed from longer strands of DNA.

While the potential for synthesis of tangled patterns may seem a nuisance, they offer interesting possibilities for downstream materials. One obvious feature of tangled structures is their relative compact volume compared with their untangled counterparts. Thus, if entanglement can be encoded into the channel structure of catalytic or storage materials, entanglement offers an elegant solution to the search for high internal surface or free volume.

A further characteristic of the simpler tangled patterns formed by polyhedral graphs make this a potentially useful complication: chirality. Recall that the simplest tangles of polyhedral graphs are those that reticulate the torus; these are the least tangled patterns. It is therefore feasible that these can be deliberately targeted using DNA edges of suitable length. We have shown recently that these toroidal isotopes of polyhedral graphs are – without exception – structurally chiral, so that they are either right- or left-handed by virtue of their entanglement [19] (This chirality is at the supra-molecular scale, and independent of the presence of chiral helical motifs in DNA). Similarly, assembly of these tangled units into extended nets can readily give chiral nets. An example is shown in Fig. 9.

So can these graph-like and net-like patterns be cast into harder materials such as mesoporous solids? The “transcription” of DNA structures into hard siliceous materials is chemically feasible and now demonstrated for isolated DNA helices. It was first proposed by Corkery [32] and later proven experimentally by Che *et al.* [33,34]. We therefore foresee the interesting possibility of marrying the rapidly developing field of DNA materials with hard inorganic meso-materials. We propose to combine that possibility with the

developing understanding of tangled patterns that can be achieved in the presence of long strands of DNA (or other polymeric frameworks, such as MOF's) and the novel area of “tangled materials” is within sight.

Acknowledgements

These ideas are we hope our own, but they have been developed following earlier discussions with our colleagues in Canberra, namely Toen Castle, Myfanwy Evans, Stuart Ramsden and Vanessa Robins, whom we thank. We also acknowledge discussions on the topic with Davide Proserpio (Milan) and Michael O'Keeffe (Arizona).

References

- [1] C.O. Dietrich-Buchecker, J.-P. Sauvage, *New J. Chem.* 16 (1992) 277–285.
- [2] C.O. Dietrich-Buchecker, J.-P. Sauvage, *Chem. Rev.* 87 (1987) 795–810.
- [3] B. Hoskins, R. Robson, *J. Am. Chem. Soc.* 112 (1990) 1546.
- [4] L. Carlucci, G. Ciani, D.M. Proserpio, *Coord. Chem. Rev.* 246 (2003) 247–289.
- [5] M. Tong, X.-M. Chen, B.-H. Ye, L.-N. Ji, *Angew. Chem. Int. Ed. Engl.* 38 (1999) 2237–2240.
- [6] M. O'Keeffe, M.A. Peskov, S.J. Ramsden, O.M. Yaghi, *Acc. Chem. Res.* 41 (2008) 1782–1789.
- [7] O. Delgado-Friedrichs, M. O'Keeffe, *Acta Crystallogr. A* 59 (2003) 351–360.
- [8] R. Scharein, K. Ishihara, J. Arsuaga, Y. Diao, K. Shimokawa, M. Vazquez, *J. Phys. A: Math. Theor.* 42 (2009) 475006.
- [9] J.H. Conway, C.M. Gordon, *J. Graph Theor.* 7 (1983) 445–453.
- [10] C. Bonneau, O. Delgado-Friedrichs, M. O'Keeffe, O.M. Yaghi, *Acta. Crystallogr. A* 60 (2004) 517–520.
- [11] T. Castle, M.E. Evans, S.T. Hyde, *New J. Chem.* 32 (2008) 1484–1492.
- [12] S. Kinoshita, *Pac. J. Math.* 42 (1972) 89–98.
- [13] C. Soteros, D. Sumners, S. Whittington, *Math. Proc. Camb. Phil. Soc.* 111 (1992) 75–91.
- [14] V. Blatov, *IUCr CompComm. Newsletter* (2006) 4–38.
- [15] S. Chung, T. Hahn, W. Klee, *Acta Cryst. A* 40 (1984) 42–50.
- [16] J.L. Gross, T.W. Tucker, *Topological Graph Theory*. Dover Publications Inc., 2001.
- [17] B. Mohar, C. Thomassen, *Graphs on Surfaces*. Johns Hopkins University Press, 2001.
- [18] S. Hyde, G. Schroeder-Turk, *Acta Cryst. A* 63 (2007) 186–197.
- [19] T. Castle, M.E. Evans, S.T. Hyde, *New J. Chem.* A63 (2007) 2107–2113.
- [20] W. Kocay (2006), Available at: <http://bkocay.cs.umanitoba.ca/g&g/K6Torus.html>.
- [21] J. Stillwell, *Mathematics and Its History*. Springer-Verlag, 1989.
- [22] O.D. Friedrichs (2008), Available at: <http://www.gavrog.org/>.
- [23] E. Rawdon, A. Dobay, J.C. Kern, K.C. Millett, M. Piatek, P. Plunkett, A. Stasiak, *Macromolecules* 41 (2008) 4444–4451.
- [24] P. Sa-Ardylen, N. Jonoska, N.C. Seeman, *J. Am. Chem. Soc.* 126 (2004) 6648–6657.
- [25] Y. Zhang, N.C. Seeman, *J. Am. Chem. Soc.* 116 (1994) 1661–1669.
- [26] F.A. Aldaye, A.L. Palmer, H.F. Sleiman, *Science* 15 (2008) 1795–1799.
- [27] J. Zheng, J.J. Birktoft, Y. Chen, T. Wang, R. Sha, P.E. Constantinou, S.L. Ginell, C. Mao, N.C. Seeman, *Nature* 461 (2009) 74–77.
- [28] J.E. Mueller, S.M. Du, N.C. Seeman, *J. Am. Chem. Soc.* 113 (1991) 6306–6308.
- [29] A. Stasiak, V. Katrich, J. Bednar, D. Michoud, J. Dubochet, *Nature* 384 (1996) 122.
- [30] H. Sleiman, private communication (2009).
- [31] T. Castle, V. Robins, S.T. Hyde, in preparation.
- [32] R. Corkery, Ordered porous materials via DNA lattice templating (2005).
- [33] C. Jin, H. Qiu, L. Han, M. Shu, S. Che, *Chem. Commun.* (2009) 3407–3409.
- [34] C. Jin, L. Han, S. Che, *Angew. Chem. Int. Ed. Engl.* 121 (2009) 9432–9436.